

Normal photoelectron diffraction studies of selenium and sulfur overlayers on Ni(011) and Ni(111)

D. H. Rosenblatt, S. D. Kevan,* J. G. Tobin, R. F. Davis,[†] M. G. Mason,[‡]
D. R. Denley,[§] and D. A. Shirley

*Materials and Molecular Research Division, Lawrence Berkeley Laboratory,
and Department of Chemistry, University of California, Berkeley, California 94720*

Y. Huang** and S. Y. Tong

*Department of Physics and Surface Studies Laboratory, University of Wisconsin-Milwaukee,
Milwaukee, Wisconsin 53201*

(Received 14 April 1982)

Normal photoelectron diffraction was used to determine the structure of $c(2\times 2)$ S and $c(2\times 2)$ Se on Ni(011) and of four different overlayers of Se on Ni(111). For $c(2\times 2)$ Se on Ni(011), Se bonds in the hollow site, whereas for $c(2\times 2)$ S on Ni(011), it is difficult to choose between the hollow and the top sites. For both a low coverage, disordered Se overlayer and an annealed $p(2\times 2)$ Se overlayer on Ni(111), Se was found to be situated in those threefold hollow sites which have a vacancy below them in the second layer. In the case of an unannealed $p(2\times 2)$ Se overlayer on Ni(111), the Se is adsorbed in approximately equal amounts in the top and hollow sites.

I. INTRODUCTION

Normal photoelectron diffraction (NPD) has been shown to be an accurate method of determining the structure of atomic¹⁻³ and molecular⁴ overlayers on single-crystal metal surfaces. In an NPD experiment the photoemission intensity of an adsorbate core level is measured normal to the surface as a function of photoelectron kinetic energy. Final-state diffraction phenomena superimpose modulations on the atomic cross section of the core level. These modulations contain structural information, which can be obtained implicitly,¹⁻⁶ by comparison of experimental and calculated NPD curves, or explicitly,^{1,7} utilizing the Fourier transformation in a manner similar to its use in extended x-ray absorption fine structure (EXAFS). The structural parameter derived from an NPD experiment is d_{\perp} , the perpendicular spacing between the adsorbate and top substrate layers.

In this paper we report applications of the NPD technique to two systems which have not been previously studied by any structural technique— $c(2\times 2)$ Se on Ni(011) and selenium adsorbed on Ni(111). Four different overlayers of Se on Ni(111) were studied and theoretical analyses are presented below. Two of these overlayers exhibit more complex NPD curves than would be expected from a Se atom in a single adsorption site. Theoretical analysis of one of these cases indicates that the selenium atom is adsorbed in two different

sites. For $c(2\times 2)$ Se on Ni(011), our NPD data clearly suggest adsorption of selenium in the hollow site with $d_{\perp} = 1.10$ Å. We also studied the adsorption of $c(2\times 2)$ S on Ni(011). An excellent theory-experiment fit for the hollow site at $d_{\perp} = 0.94$ Å was obtained, in agreement with the earlier low-energy electron diffraction (LEED) result.⁸ However, our experimental data range is too limited to rule out the top site unambiguously.

Section II contains experimental information. In Sec. III we briefly describe the multiple-scattering calculations used to fit the experimental data. In Sec. IV we present the NPD data and a discussion of the surface structures which are derived, and in Sec. V a few conclusions about this work are given.

II. EXPERIMENTAL

All data reported here were obtained with an angle-resolved photoemission (ARP) spectrometer described elsewhere.⁹ The spectrometer has LEED and Auger electron spectroscopy capabilities, as well as an adsorbate introduction system which allows for effusive beam dosing. The base pressure of the vacuum chamber was 2×10^{-10} Torr during all measurements. The pressure rose to as high as 5×10^{-9} Torr during effusive beam dosing. The Ni(011) and Ni(111) crystals were oriented to within 1° of the appropriate crystal faces. Both crystals were cleaned by hot (1025 K) and room-

temperature cycles of argon-ion sputtering followed by annealing to 875 K, resulting in surfaces essentially free of impurities with sharp (1×1) LEED patterns. The $c(2 \times 2)$ S and Se overlayers on Ni(011) were prepared by exposing the clean Ni(011) crystal to 10–15 L of H_2S and H_2Se , respectively, with the crystal at 300 K.¹⁰ A $p(2 \times 2)$ Se overlayer (taken to be 0.25 monolayer) on Ni(111) with a sharp LEED pattern was obtained by cooling the sample to 120 K, exposing it to about 2 L of H_2Se , and then annealing the sample to 500 K.¹⁰ A $p(2 \times 2)$ LEED pattern was also obtained by exposing Ni(111) to H_2Se with the sample at 120 K and not allowing it to warm up.¹¹ The quality of the latter LEED pattern was poorer, however. The $(\sqrt{3} \times \sqrt{3})R30^\circ$ Se overlayer (0.5 monolayer) was prepared by increasing the exposure to 5 L of H_2Se . The $(\sqrt{3} \times \sqrt{3})R30^\circ$ LEED spots were weak and there was a substantial diffuse background. Finally, a low-coverage (0.1-monolayer) overlayer of Se on Ni(111) was produced with a 1-L exposure. This overlayer gave a LEED pattern indicative of a disordered overlayer (only LEED spots due to the substrate were present). The coverage of the latter two overlayers was determined by comparing their Se $3d$ photoemission intensity (normalized by Ni $3p$ intensity) to that of the $p(2 \times 2)$ overlayer (assumed to be 0.25 monolayer).

The experiments were performed on Beam Line I-1 at the Stanford Synchrotron Radiation Laboratory (SSRL). Low-resolution ARP spectra were taken of the Se $3d$ and S $2p$ levels, which have binding energies of 62 and 170 eV below the vacuum level, respectively. Spectra were taken at photon energy intervals of 3 eV. The angle-resolved relative intensities of these levels were computed by calculating the area of the core-level peaks (after background subtraction) and adjusting for photon flux and analyzer transmission. The kinetic-energy range of the resulting NPD curves was generally 20–200 eV for the Se $3d$ studies and was 20–150 eV for the one S $2p$ system discussed below. Experimental geometries are indicated in the figures.

III. THEORY

We used a Green's-function multiple-scattering method⁵ to calculate the NPD intensity versus energy (IE) spectra. Wave functions for Se $3d$ and S $2p$ were generated from self-consistent $X\alpha$ scattered-wave calculations of Ni_5Se and Ni_5S clusters. Inputs to the multiple-scattering calculation

include Ni phase shifts from the self-consistent potential of Wakoh,¹² and Se or S phase shifts from the same $X\alpha$ scattered-wave calculations that generated the initial-state wave functions. The inner potentials used were $V_0 = 11.2$ eV for Se and $V_0 = 9.95$ eV for S overlayers.

Calculations were done with the overlayer placed at high-symmetry sites, i.e., the top, hollow, and bridge sites. At each site, 8 to 12 interlayer spacings (d_\perp) between the overlayer and the top substrate layer were tried. Calculations were carried out with increments in d_\perp of 0.02 Å for S and Se on Ni(011) and 0.05 Å for Se on Ni(111). In Figs. 3–7, calculated curves are shown only at selected d_\perp values.

IV. RESULTS AND DISCUSSION

A. Selenium overlayers on Ni(111)

In this section we present NPD results for four different overlayers of selenium adsorbed on Ni(111). The lowest coverage studied was a disordered overlayer. We also studied the two ordered overlayers for which LEED patterns have been previously observed; i.e., the $p(2 \times 2)$ and $(\sqrt{3} \times \sqrt{3})R30^\circ$ structures. The selenium on Ni(111) system is of special interest both because there has been no structural determination by LEED intensity analysis or any other technique to date and because of the possibility that multiple adsorption sites might be present at certain selenium coverages. Structural studies of adsorbates on fcc (111) surfaces are also of interest because of the existence of two types of threefold hollow sites. Half of the threefold hollow sites on a Ni(111) surface layer have substrate atoms directly below them in the second layer, while the other half have vacancies in the second layer. In this section we show that NPD is sensitive to these two types of threefold hollow sites for selenium adsorbed on Ni(111).

The experimental geometry for all the NPD measurements of the Se-Ni(111) system is shown in Fig. 1. Figure 1(a) shows that the photon vector potential (\hat{A}) and the direction of emission (e^-) lie in the plane defined by the $[111]$ and $[\bar{2}11]$ directions. The orientation of the atoms on the Ni(111) face is shown in Fig. 1(b). The positions of the four possible high-symmetry adsorption sites for Se on Ni(111) are shown with respect to the first two layers of substrate atoms in Fig. 1(c). Using hard-sphere radii to determine the expected values of the

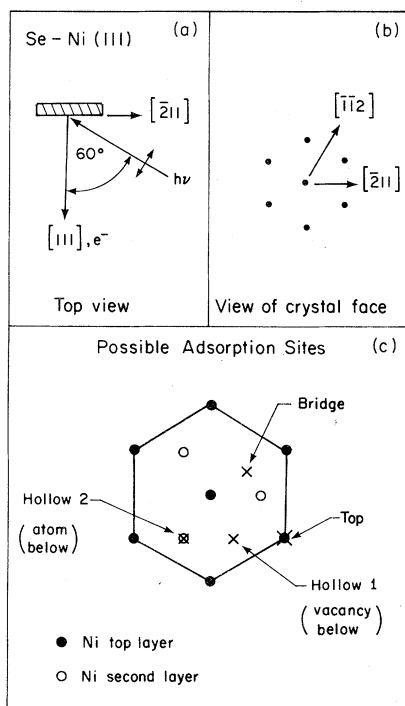


FIG. 1. (a) Experimental arrangement for all Se-Ni(111) studies, showing the orientation of the incident photon beam ($h\nu$), the photon vector potential (\vec{A}), and the outgoing photoelectron direction (e^-). (b) View of the Ni(111) crystal face showing the orientation of the first layer of atoms. (c) Positions of the four possible high-symmetry adsorption sites with respect to the first and second layer of substrate atoms.

structural parameter d_{\perp} , one obtains $d_{\perp} = 1.85 \text{ \AA}$ for both hollow sites, $d_{\perp} = 2.00 \text{ \AA}$ for the bridge site, and $d_{\perp} = 2.30 \text{ \AA}$ for the top site. Because of the close-packed arrangement of atoms on the Ni(111) surface, the d_{\perp} values for the three sites, as predicted by a hard-sphere model, are much closer to one another than for the Ni(001) and Ni(011) surfaces.

In Fig. 2, all four experimental NPD curves for Se-Ni(111) are plotted. The lowest coverage studied, shown at the bottom, was a disordered selenium overlayer, estimated to be 0.1 monolayer. The second curve from the bottom in Fig. 2 was obtained from a $p(2 \times 2)$ overlayer (0.25 monolayer). Both of these overlayers had been heated to 500 K after the H_2Se exposure and then cooled to 120 K during NPD data acquisition. Because the $p(2 \times 2)$ overlayer was heated (resulting in an improvement of the $p(2 \times 2)$ LEED pattern), we refer to it as the "annealed" $p(2 \times 2)$ overlayer. Just as in a previous study of Se on Ni(001) carried out in our laboratory,¹³ the NPD data for the low-coverage and

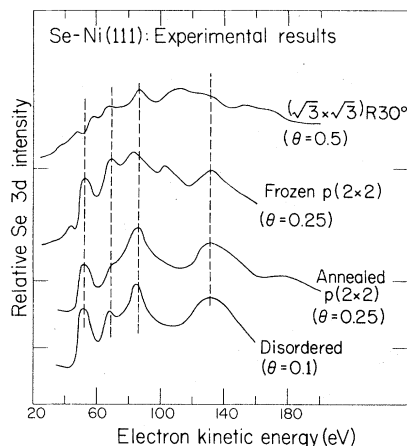


FIG. 2. Experimental NPD results for the four overlayers of Se on Ni(111) studied.

annealed $p(2 \times 2)$ overlayers of Se on Ni(111) are quite similar. Slight differences are seen in the peak at 65-eV kinetic energy, which are possibly the result of the experimental difficulties involved with lower coverages and the presence of a nickel Auger peak in that energy region.

In Fig. 3, the experimental results from the annealed $p(2 \times 2)$ Se-Ni(111) surface are compared to theoretical calculations for the four possible high-symmetry adsorption sites. Excellent agreement is found for hollow site 1 (with a vacancy below) and $d_{\perp} = 1.80 \text{ \AA}$. This value is slightly smaller (0.05 \AA) than the d_{\perp} value obtained by using hard-sphere radii derived from the $c(2 \times 2)$ Se-Ni(001) surface.² The only experimental peak which shows a mismatch with theory is the first peak (~ 50 -eV kinetic energy), and previous NPD work has indicated that there are substantial problems with both

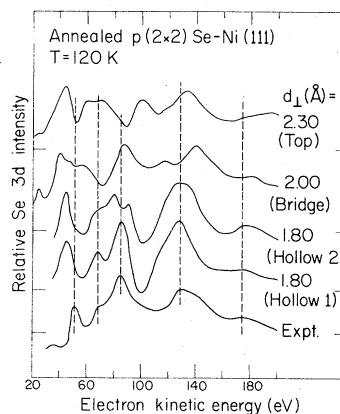


FIG. 3. Experimental NPD curve for the annealed $p(2 \times 2)$ Se-Ni(111) system compared with calculated curves.

theory and experiment in this energy region.¹⁷ Fair but definitely inferior agreement is also found for hollow site 2 (atom below) and $d_{\perp} = 1.80 \text{ \AA}$. Poor agreement is found for the top site and the bridge site (the curve shown is an average over nonequivalent bridge-site curves). The main difference between the theoretical curves for the two hollow sites is found in the structure of the peak around 90 eV. Just as in the experimental curve, there is a single peak in the curve for hollow site 1 whereas that peak is split into two peaks separated by 12 eV in the case of hollow site 2. The other regions of the hollow-site 1 curve also agree slightly better with experiment than the hollow-site 2 curve does. Unfortunately, the differences between the two hollow-site calculated curves are not as great at $d_{\perp} = 1.80 \text{ \AA}$ as they are at other values of d_{\perp} . To demonstrate this point, the theoretical hollow-site NPD curves for $d_{\perp} = 1.60 \text{ \AA}$ and 2.00 \AA are shown in Fig. 4. The differences between sites 1 and 2 are significant at many energies for both cases. Certain peaks are shifted by 5–10 eV from one hollow site to the other. The accuracy of the d_{\perp} value was determined with a procedure outlined earlier.¹ We find $d_{\perp} = 1.80 \pm 0.04 \text{ \AA}$ for this case. If one assumes the bulk structure for the surface layer of nickel atoms, the Se–Ni bond length is $2.31 \pm 0.03 \text{ \AA}$.

We have presented a case in which NPD has been able to differentiate between a selenium atom in two different sites at the same d_{\perp} . By contrast, surface EXAFS¹⁴ would not be particularly valuable for this case if only the first-nearest-neighbor

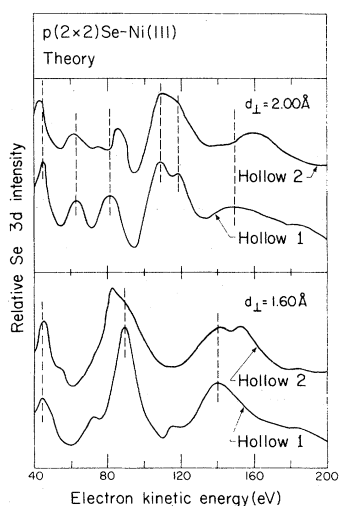


FIG. 4. Comparison of calculated curves for a $p(2 \times 2)$ Se-Ni(111) overlayer situated in hollow site 1 and in hollow site 2 at two different d_{\perp} spacings.

distance were obtained, because that distance is essentially the same for the two hollow sites. Polarization-dependent surface EXAFS¹⁵ can determine the surface-atom coordination number, allowing one to distinguish between top, bridge, and hollow sites, but not between the two different types of threefold hollow sites. Second- and third-nearest-neighbor distances¹⁶ would have to be obtained to determine the site unambiguously with surface EXAFS. Azimuthal photoelectron diffraction (APD), on the other hand, could be applied successfully to this problem because of its sensitivity to the orientation of the substrate atoms relative to the adsorbate atoms. This was demonstrated in a recent APD study of the iodine on Ag(111) system,^{17,18} in which theoretical APD curves by Kang *et al.*¹⁸ for the two threefold hollow sites were similar in structure but out of phase by 60° . Comparison of these theoretical curves to the experimental data of Farrell *et al.*¹⁷ led to the conclusion that the iodine atoms occupy both hollow sites at low coverages. Unfortunately, APD was not particularly sensitive to the d_{\perp} spacing in that experiment, and in general APD has difficulty in determining d_{\perp} if the adsorbate is located substantially above the surface.¹⁹

The determination of hollow site 1 with $d_{\perp} = 1.80 \text{ \AA}$ as the geometry of the annealed $p(2 \times 2)$ Se overlayer on Ni(111) also, in effect, provides a structural determination of the low-coverage, disordered overlayer shown in Fig. 2, as the two experimental curves are almost identical. This is an important result, as it again demonstrates that NPD can deal with disordered systems.² It is not surprising that the small number of selenium atoms on the surface in the low-coverage regime (0.1 monolayer) find the same site to be energetically favorable as in the 0.25-monolayer coverage. In both cases, there is some distance between the selenium atoms and consequently adatom-adatom interactions should be fairly small. For this disordered Se overlayer on Ni(111), the selenium is situated in hollow site 1 (vacancy below) with $d_{\perp} = 1.80 \pm 0.05 \text{ \AA}$. The Se–Ni bond length is $2.31 \pm 0.04 \text{ \AA}$.

Evidence for the presence of multiple adsorption sites was obtained from a temperature dependence study of the $p(2 \times 2)$ Se-Ni(111) system. The annealed $p(2 \times 2)$ Se overlayer for which an NPD curve is shown in Fig. 2 was prepared by heating the surface to 500 K after the H_2Se exposures. A second $p(2 \times 2)$ overlayer, which will be referred to as the frozen surface, was prepared at 120 K and held at that temperature before and during the

NPD study. Both samples gave good $p(2 \times 2)$ LEED patterns, although that of the annealed surface exhibited sharper spots. The NPD result for the frozen-surface is also shown in Fig. 2. Both the annealed and the frozen-surface results were reproducible on three separate surface preparations. The frozen surface gave peaks within a few eV of those observed from the annealed $p(2 \times 2)$ surface, but there is an additional peak in the frozen-surface NPD curve at 102-eV kinetic energy which is located in a valley of the annealed-surface curve. Visual inspection of the curves leads to the hypothesis that the Se can be frozen into multiple binding sites by performing exposures at low temperatures, and that by heating the surface, the preferred site becomes populated exclusively.

The above interpretation is borne out by the theoretical calculations. If the calculated NPD curves for $p(2 \times 2)$ Se-Ni(111) from Fig. 3 are compared to the frozen $p(2 \times 2)$ data, no single theoretical curve is able to account for all the features in the experimental curve. Consequently, a combination of two or more theoretical curves is required to produce a good theory-experiment fit. Inspection of these curves indicated that several of the peaks in the hollow-site 1, hollow-site 2, and top-site curves correspond fairly closely with peaks in the experimental curve. This led to a more quantitative attempt to determine the structure by adding together the three curves with different weightings. Owing to the relative closeness of the two hollow-site curves in comparison to the top-site curve, an average of the two hollow-site curves was taken. This average (called "hollow") is shown in Fig. 5, along with the top-site curve (reproduced from Fig. 3). If the hollow- and top-site curves are normalized (by photoemission intensity per selenium atom) and added together with equal weighting, the resulting NPD curve ("average of top and hollow") shows very good agreement with experiment, as indicated in Fig. 5. This curve actually contains the following contributions (after normalization): 50% top site ($d_1 = 2.30 \text{ \AA}$), 25% hollow site 1 ($d_1 = 1.80 \text{ \AA}$), and 25% hollow site 2 ($d_1 = 1.80 \text{ \AA}$). Note that the extra peak in the frozen $p(2 \times 2)$ curve at 102 eV is reproduced, as well as the energy difference between the two large peaks at 81 and 132 eV (51 eV). The difference between those same peaks in the averaged hollow-site data is only 43 eV, so the top-site contribution is important in establishing a good fit for those two peaks as well. It is reasonable to expect that both hollow site 2 and the top site will be occupied under these conditions, because at 120 K, atoms can be frozen into

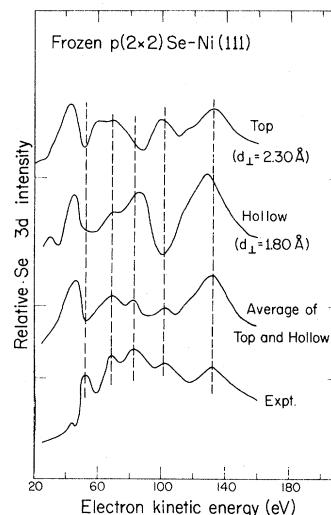


FIG. 5. Experimental NPD curve for the frozen $p(2 \times 2)$ Se-Ni(111) surface compared with calculated curves.

sites which are not as energetically favored as hollow site 1. We conclude that there are roughly an equal number of top- and hollow-bonded selenium atoms on the surface. This is the first evidence from NPD for multiple-site behavior.

Finally, the higher-coverage $(\sqrt{3} \times \sqrt{3})R 30^\circ$ Se on Ni(111) system was also studied. The LEED patterns that were observed were not as sharp as those seen by other workers,¹¹ probably because the coverage of 0.5 monolayer is considerably greater than the 0.33-monolayer coverage for a perfect $(\sqrt{3} \times \sqrt{3})R 30^\circ$ overlayer. Unfortunately, no coverage between 0.25 and 0.5 monolayers was studied. As shown in Fig. 2, the $(\sqrt{3} \times \sqrt{3})R 30^\circ$ overlayer showed a smaller NPD effect than the other overlayers studied. The size of the modulations is so small in this case that it is very difficult to make an accurate structural determination. It appears that either three or more high-symmetry sites are significantly occupied, or that the coverage is so high that the selenium atoms are occupying low-symmetry sites as well. Calculations for the $(\sqrt{3} \times \sqrt{3})R 30^\circ$ overlayer were carried out, but no successful fit with the experimental data was obtained by assuming either a single high-symmetry adsorption site or a combination of two such sites.

B. The $c(2 \times 2)$ selenium and sulfur overlayers on Ni(011)

In this section we report the results of the first NPD studies of adsorption on a (011) surface. The

adsorbates Se and S were chosen in part because of the ease in which the $c(2 \times 2)$ overlayers can be prepared on Ni(011) and the relatively large photoemission cross sections of the Se $3d$ and S $2p$ levels.

A LEED pattern for the $c(2 \times 2)$ Se overlayer on Ni(011) has been observed¹⁰ but no intensity analysis has been published. The experimental NPD curve for this system is presented in Fig. 6, along with calculated curves for selenium in the hollow site ($d_{\perp} = 1.10 \text{ \AA}$), the long-bridge site ($d_{\perp} = 1.54 \text{ \AA}$), the short-bridge site ($d_{\perp} = 2.00 \text{ \AA}$), and the top site ($d_{\perp} = 2.30 \text{ \AA}$). The experimental geometry is indicated in the figure. Excellent agreement is found for the hollow site, with poor agreement for all other sites. Thus, NPD produces a clear preference for selenium in the hollow site with $d_{\perp} = 1.10 \text{ \AA}$, with an uncertainty of $\pm 0.04 \text{ \AA}$. The Se-Ni bond length is $2.42 \pm 0.02 \text{ \AA}$. It should be emphasized that this is the first structural determination of a selenium overlayer on Ni(011).

The structure of the $c(2 \times 2)$ S overlayer on Ni(011) has been studied previously by LEED intensity analysis. The sulfur was found to bond in the hollow site above the (011) surface with $d_{\perp} = 0.93 \text{ \AA}$.⁸ The experimental NPD curve for the system is shown in Fig. 7. Above the experimental data, theoretical curves for the hollow site ($d_{\perp} = 0.94 \text{ \AA}$), the long-bridge site ($d_{\perp} = 1.30 \text{ \AA}$), the short-bridge site ($d_{\perp} = 1.80 \text{ \AA}$), and the top site ($d_{\perp} = 2.20 \text{ \AA}$) are plotted. Excellent agreement is found for both the hollow site and the top site, because the theoretical curves for those two sites are very similar in the energy range studied, i.e., 20–150 eV. Extending the curve to higher kinetic energies would have allowed us to choose between

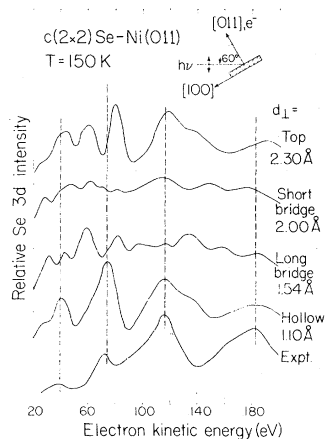


FIG. 6. Experimental NPD results for $c(2 \times 2)$ Se-Ni(011) compared with calculated curves for the experimental arrangement shown.

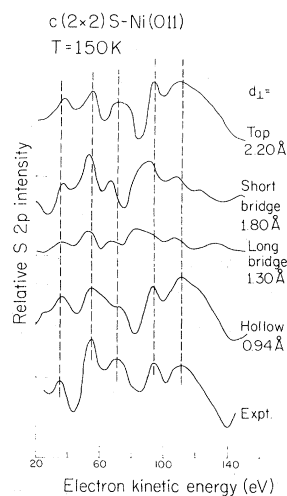


FIG. 7. Experimental NPD curve for $c(2 \times 2)$ S-Ni(011) compared with calculated curves. The experimental arrangement is the same as in Fig. 6.

hollow and top sites, as the theoretical curves do show differences above 150 eV. This case provides an example of an accidental coincidence between two theory curves over a short energy range,²⁰ and shows the need to take as wide a data range as possible. This work therefore only partially confirms the LEED result in the sense of excluding both bridge sites, but a unique structure would require a longer data range, with more NPD peaks, to distinguish between the hollow and the top site. The accidental coincidence could also be obviated by taking photoelectron diffraction curves at off-normal emission angles.²¹

V. CONCLUSIONS

In this paper we have reported the results of a series of experiments designed to further assess the value of NPD as a surface-structure-sensitive technique. Some conclusions are given below:

- (1) NPD has been used successfully to study systems that have not yet been studied by any other accurate structural technique.
- (2) NPD seems to be particularly well suited for studying disordered adsorbate systems and systems which have two-dimensional order but contain domains of two adsorption sites.
- (3) NPD has the potential to select between sites which have the same geometry with respect to the first substrate layer but have a different geometry with respect to the second layer.

(4) The importance of taking an extended range of data has been demonstrated by the inability of NPD to select between two different sites which have similar theoretical curves over a short energy range.

ACKNOWLEDGMENTS

We wish to acknowledge Mrs. Winifred Heppler for the preparation of the nickel crystals. One of us (J.G.T.) acknowledges support by an NSF post-

graduate fellowship. This work was supported by the Director, Office of Energy Research, Office of Basic Energy Sciences, Chemical Sciences Division of the U.S. Department of Energy under Contract No. DE-AC03-76SF00098. It was performed at the Stanford Synchrotron Radiation Laboratory, which is supported by the NSF through the Division of Materials Research. Work at the University of Wisconsin-Milwaukee was supported by NSF Grant No. DMR 8101203 and PRF Grant No. 11584-AC 5,6.

*Permanent address: Bell Laboratories, Murray Hill, NJ 07974.

†Permanent address: Research Laboratories, Polaroid Corporation, Waltham, MA 02154.

‡Permanent address: Research Laboratories, Eastman Kodak Company, Rochester, NY 14650.

§Permanent address: Westhollow Research Center, Shell Development Co., Houston, TX 77001.

**Permanent address: Chinese Academy of Sciences, Institute of Physics, Peking, People's Republic of China.

¹D. H. Rosenblatt, J. G. Tobin, M. G. Mason, R. F. Davis, S. D. Kevan, D. A. Shirley, C. H. Li, and S. Y. Tong, *Phys. Rev. B* **23**, 3828 (1981), and references therein.

²S. D. Kevan, D. H. Rosenblatt, D. R. Denley, B.-C. Lu, and D. A. Shirley, *Phys. Rev. B* **20**, 4133 (1979).

³C. H. Li and S. Y. Tong, *Phys. Rev. Lett.* **42**, 901 (1979).

⁴S. D. Kevan, R. F. Davis, D. H. Rosenblatt, J. G. Tobin, M. G. Mason, D. A. Shirley, C. H. Li, and S. Y. Tong, *Phys. Rev. Lett.* **46**, 1629 (1981).

⁵C. H. Li, A. R. Lubinsky, and S. Y. Tong, *Phys. Rev. B* **17**, 3128 (1978).

⁶S. Y. Tong and C. H. Li, *Crit. Rev. Solid State Sci.* **10**, 209 (1981).

⁷Z. Hussain, D. A. Shirley, S. Y. Tong, and C. H. Li, *Proc. Natl. Acad. Sci. U.S.A.* **78**, 5293 (1981).

⁸J. E. Demuth, D. W. Jepsen, and P. M. Marcus, *Phys. Rev. Lett.* **32**, 1182 (1974).

⁹S. D. Kevan and D. A. Shirley, *Phys. Rev. B* **22**, 542 (1980).

¹⁰G. E. Becker and H. D. Hagstrom, *Surf. Sci.* **30**, 505 (1972).

¹¹T. Capehart and T. N. Rhodin, *J. Vac. Sci. Technol.* **16**, 594 (1979).

¹²S. Wakoh, *J. Phys. Soc. Jpn.* **20**, 1894 (1965).

¹³S. D. Kevan, J. G. Tobin, D. H. Rosenblatt, R. F. Davis, and D. A. Shirley, *Phys. Rev. B* **23**, 493 (1981).

¹⁴P. H. Citrin, P. Eisenberger, and R. C. Hewitt, *Phys. Rev. Lett.* **41**, 309 (1978).

¹⁵P. H. Citrin, P. Eisenberger, and R. C. Hewitt, *Phys. Rev. Lett.* **45**, 1948 (1980).

¹⁶A second-nearest-neighbor distance has recently been observed. [S. Brennan, J. Stohr, and R. Jaeger, *Phys. Rev. B* **24**, 4871 (1981)].

¹⁷H. H. Farrell, M. M. Traum, N. V. Smith, W. A. Royer, D. P. Woodruff, and P. D. Johnson, *Surf. Sci.* **102**, 527 (1981).

¹⁸W. W. Kang, C. H. Li, and S. Y. Tong, *Solid State Commun.* **36**, 149 (1980).

¹⁹P. J. Orders, R. E. Connelly, N. F. T. Hall, and C. S. Fadley, *Phys. Rev. B* **24**, 6163 (1981).

²⁰C. H. Li and S. Y. Tong, *Phys. Rev. B* **19**, 1769 (1979).

²¹D. H. Rosenblatt, S. D. Kevan, J. G. Tobin, R. F. Davis, M. G. Mason, D. A. Shirley, J. C. Tang, and S. Y. Tong, *Phys. Rev. B* (in press).